



Improvement of a novel polymeric membrane performance by adding alumina powder for seawater desalination

Hanan Ajari^a, Khaoula Hidouri^{a,*}, Hiba Akrou^a, Fatma Khaled^a, Benhmidene Ali^a, Béchir Chaouachi^a, Qusay Alsalhy^b

^aResearch laboratory: Energy, Water, Environment and Processes, National School of Engineers of Gabes (E.N.I.G), University of Gabes, Tunisia, emails: khaoula2013@yahoo.fr (K. Hidouri), haneneajari@gmail.com (H. Ajari), akrouthiba@gmail.com (H. Akrou), fatma90khaled@gmail.com (F. Khaled), ali.benhmidene@gmail.com (B. Ali), bechir.chaouachi@enig.rnu.tn (B. Chaouachi)

^bMembrane Technology Research Unit, Department of Chemical Engineering, University of Technology-Iraq, Alsinaa Street 52, Baghdad 10066, Iraq, email: qusay.f.abdulhameed@uotechnology.edu.iq

Received 18 June 2023; Accepted 1 December 2023

ABSTRACT

In this study, a composite membrane was prepared from recycled low-density polyethylene (R-LDPE), thus helping to lighten plastics' load on the environment, while the powder of alumina was used to enhance the membrane contact angle, its porosity, and its mechanical properties. The membrane preparation was made by means of the thermally induced phase separation method by using the butyl acetate as a solvent, hexane as a non-solvent, and the alumina as an additive. The membrane crystalline property was assessed *via* the Fourier-transform infrared spectroscopy. The membrane characteristics were then investigated in terms of thickness, contact angle, pore size, porosity, mechanical test, bubble point pressure, atomic force microscopy, and scanning electron microscopy analysis. The results revealed that the addition of alumina had an important role in improving membrane structure, properties and therefore its performance. The evaluation of the R-LDPE-alumina membrane showed that it has a good porosity, good hydrophobicity, and better mechanical properties. The obtained membranes were also applied to the vacuum membrane distillation to test their performance.

Keywords: Recycled low density polyethylene; Alumina; Membrane; Hydrophobic; Thermally induced phase separation

1. Introduction

Water is a basic requirement in every human being's daily life. Freshwater scarcity is a big problem caused by pollution caused by human interruption, urbanization, and especially waste. In fact, the post-consumer waste generation in the United States as an example reached 216 million tons of solid waste per year in the year 2000, posing serious environmental and engineering challenges. Moreover, the decomposition of these wastes leads to the release of toxins contained in water sources, whether underground or surface, and contamination of the soil in a way that affects the

food cycle along with contamination of drinking water and thus poses risks to the safety of people. Therefore, recycling materials reduces the need to deplete more natural resources to extract new raw materials. On the other hand, there is another issue that the world is experiencing, the issue of the scarcity of fresh water. Adding the global population growth that will reach, according to the UN, 9.8 billion people in 2050 and each person needs from 2–3 L/d of drinking water [1]. Consequently, desalination becomes a necessity for this important issue [2,3]. For this, the research community is concentrating on water filtration and desalination to

* Corresponding author.

produce large amounts of purified water in a short period of time and at a low cost. Many technologies were carried out in this context: thermal processes such as distillation (MSF, MED, MED-TC), membrane processes such as reverse osmosis (RO), and the hybrid process such as membrane distillation (MD). There are several criteria to choose which of these processes is most appropriate: cost, water quality, efficiency, and environment. Nowadays, MD is very emerging technology, and compared with the other membrane process, MD manifests as a promising alternative [4] due to its advantages such as (1) a 100% theoretical rejection factor of salts, (3) lower operating pressures than conventional pressure-driven membrane separation processes (nanofiltration, ultrafiltration, microfiltration, and RO), (4) fewer requirements on membrane mechanical properties (5) less sensitive to feed salinity for desalination. However, this process is relatively expensive because of its high-energy consumption and operating at low temperatures, which constitutes a heating constraint at temperatures above 80°C. For this, it is necessary to couple this membrane process with renewable energy such as geothermal, which the water production cost reduced from 1.22 to 0.5\$/m³ [5–10], or solar energy [11,12], and improve its high resistance to high temperatures. In this work, solar vacuum membrane distillation was investigated for water desalination. The membrane is the principal parameter making the MD process successful. The membrane must be hydrophobic and porous in order to be suited for this technique. Many researchers have used various materials to prepare hydrophobic-porous membranes such as polyvinylidene fluoride (PVDF), PTFE, PP, and PE. All these studies have shown promising results, but still, the polymer cost is very high, and the MD membranes cost can be estimated at 90\$/m² [13,14]. Therefore, in this work, recycled low-density polyethylene was used to prepare a flat sheet membrane for vacuum membrane distillation (VMD) application to solve together the scarcity of fresh water and disposal of solid waste issues. This material is used for several reasons, such as being very cheap, hydrophobic in nature, small surface energy of 28–33·10⁻³ N/m that is like PVDF and PP, good chemical stability, and very low thermal conductivity [15–17].

In addition, composite membranes have gotten a lot of attention today because of their flexibility in having more than one layer and using a variety of materials to form the membrane. In this present paper, a composite membrane was prepared using recycled low-density polyethylene (R-LDPE), thus helping to lighten plastics' load on the environment, and the powder of alumina which it can be reinforce these membranes and improve its properties for better MD efficiency. PE membranes for MD can be made from melt-extrusion/cold-stretching methods [18]. Thermally induced phase separation (TIPS) has been used intensively to make microporous membranes since the 1980s. It was introduced firstly by Castro, and patented by several people for the preparation of microporous polymeric membranes. Besides, the use of TIPS method in the preparation of PE membranes is very limited. For this, in the present study flat sheet membrane was made by the TIPS method.

The objective of this work is to prepare a novel polymeric membrane based on R-LDPE, to improve its performance by adding alumina powder, and to test it in solar

vacuum membrane distillation (SVMD) for seawater and brackish water desalination.

2. Experimental set-up

2.1. Materials

Recycled low-density polyethylene polymer (R-LDPE) named Lacten (ATO) or lugden (BASF) (0.928 g/cm³, $M_w = 45,000$ g/mol) was supplied by a plastic manufacturing company located in Gabes (Tunisia). Commercial sodium hydroxide, butyl acetate, kerosene, ethanol, hexane, and methanol were purchased by Sigma-Aldrich (Allemagne).

2.2. Fabrication of AL/R-LDPE composite membrane

The recycled LDPE was cleaned and rinsed in the first stage. To eliminate contaminants, the recycled polymer was washed using sodium hydroxide and distilled water in this particular instance. Then, flat sheet membranes were made initially by preparing the homogeneous solution (the collodion); mixing R-LDPE (8 wt.%) in the solvent which is the butyl acetate in this case. Then the powder of alumina was added to the polymer solution. The resulting solution was stirred for 5 h at 120°C until complete dissolution of the polymer was achieved. Flat sheet LDPE membranes were prepared as shown in Fig. 1 by casting the dope solution on a glass plate (at 120°C) by means of a manual casting knife with a reservoir (Elcometer 3700/1 Doctor Blade, Germany; adjustable gap size in the range 30–4,000 μm) with a 400 μm gap. The nascent film was exposed to atmospheric conditions for 5 min; then it was immersed in a hexane bath and then in the water for 24 h to assure the solvent extraction from the membrane. Finally, the membrane was dried at ambient temperature before using it for testing. The composition of the polymer, alumina powder and the solvent, the characteristic of the membrane casting are reported in Table 1.

2.3. Membrane topography atomic force microscopy, hydrophobicity

The surface properties of flat sheet membrane were evaluated using an atomic force microscope (Bruker Nanoscope III Device (USA), France). The 3D surface topography of the membrane surface was obtained and the surface roughness was then calculated. It is described by Eq. (1) [19]:

$$Ra = \frac{1}{L_x L_y} \int_0^{L_x} \int_0^{L_y} |Z(x, y)| dx dy \quad (1)$$

where Ra: is the roughness, $Z(x, y)$: is the surface relative to the median plane, L_x, L_y : are the dimensions of the area.

The membrane contact angle (CA) was assessed using the sessile drop method. For this, a drop of bi-distilled water was deposited on the membrane by means of a micro syringe. Then the contact angle was measured using a goniometer (CAM100 Instrument, Italy). For the membrane, 6 different places were measured; the average value and then the corresponding standard deviation were calculated.

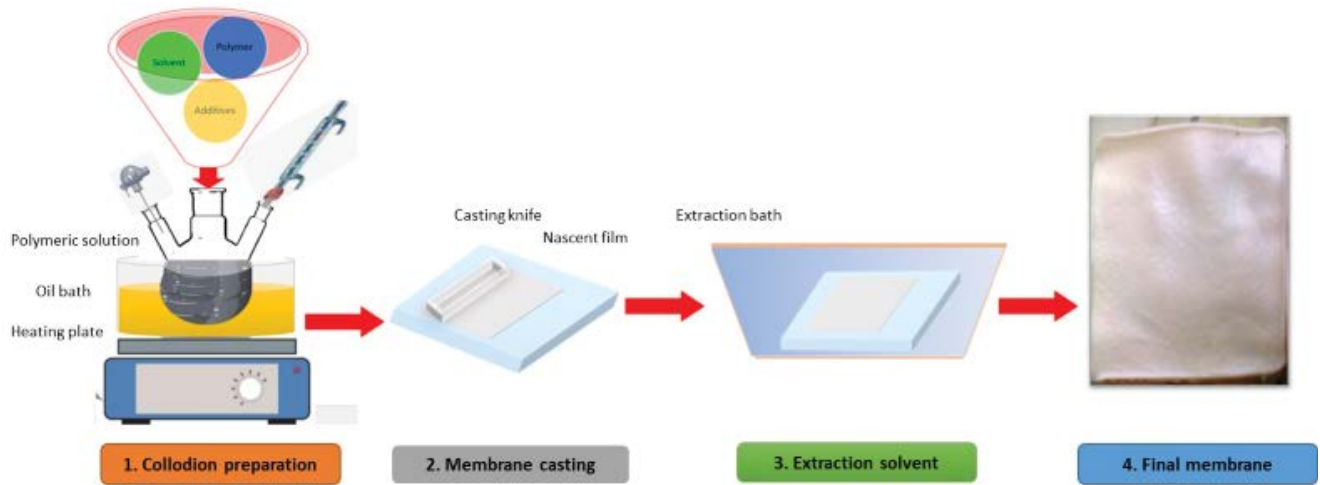


Fig. 1. Experimental set-up of the preparation of flat sheet membranes.

Table 1

Composition of the R-LDPE, alumina powder, solvent, and the different characteristics of membrane casting

Type of membrane	R-LDPE-alumina
LDPE (wt.%)	8
Alumina powder (wt.%)	5
Butyl acetate (wt.%)	87
Temperature of the solution (°C)	120
Time of stirring (h)	5
Gap size of the casting knife (μm)	400

2.4. Membrane morphology, porosity, pore size and bubble point

The membrane surface was studied through examining the scanning electron microscopy (SEM) images using SEM type of (Zeiss EVO MA10, Switzerland). Membranes cross sections were set by freeze fracturing the samples in liquid nitrogen, to produce a clean brittle fracture. To make the membrane samples conductive, a thin film of gold was put on before the SEM test.

The overall porosity of the membrane can be calculated by Eq. (2) [19]:

$$\varepsilon\% = \frac{(w_w - w_d) / \rho_k}{(w_w - w_d) / \rho_k + w_d / \rho_p} \times 100 \quad (2)$$

where w_w is the mass of the wet sample (g), w_d is the mass of the dry sample (g), ρ_p is the density of the polyethylene (0.92 g/cm³) and ρ_k is the density of the kerosene (0.82 g/cm³).

For this, the dried resulting membranes were cut into three different pieces, weighed, and then immersed in kerosene. After 24 h, the samples were removed and cleaned to remove the residual kerosene on the surfaces of the membranes and reweighed.

Average pore size and the bubble point of the flat sheet membranes were evaluated by wet/dry process using pore wick as wetting liquid (surface tension 16 dyne/cm) and a Capillary Flow Porometer (CFP 1500 AEXL, Porous Materials

Inc., USA). First, the bubble point was identified when the first bubble of pure nitrogen was allowed into the membrane that's exactly where the nitrogen pressure will be bigger than the capillary flow of the fluid inside the largest pore. Then, the pressure was continuing to increase until the drying of the flat sheet membrane means that all the pores were empty of the pore wick. According to the nitrogen flow rates through the wet and dry membranes, the attached software then calculated the pore size. Fadhil et al. [20] report on the measurements in greater detail.

2.5. Tensile properties

The mechanical properties of the flat sheet membranes were determined using a (ZWICK/ROELL Z 2.5 Test Unit, ITM-CNR Italy). Three samples (1 cm² × 5 cm²) were tested for each membrane. Each one was stressed, in unidirectional strain, at a constant rate of 5 mm/min. The tensile strength, strain at break, elastic or Young's modulus and the breaking elongation were determined.

2.6. Membrane applications: VMD experiments

The VMD experiments were carried out using the laboratory system shown schematically in Fig. 2. The membrane was placed between the upper compartment (feed side) and the lower compartment (permeate side). The effective area of the membrane was 12 cm², which was calculated based on the area of the membrane exposed to the vacuum space. The feed solution (seawater solution with 40 g/L of salinity) was circulated on the membrane upstream side and passed through a heating water bath (Carlo Gavazzi-PDI409, Tunisia) equipped with a temperature controller with accuracy ±0.1°C. During the experiments, the feed was continuously stirred at atmospheric pressure and the temperature was varied between 25°C and 90°C. The permeate side was connected to a vacuum pump to withdraw the vapor. The downstream pressure varied between 0.2 and 0.9 bar. Permeate was condensed in a cold trap immersed in liquid nitrogen and immediately the collected permeate is weighed each hour to examine the flux variation. The permeate

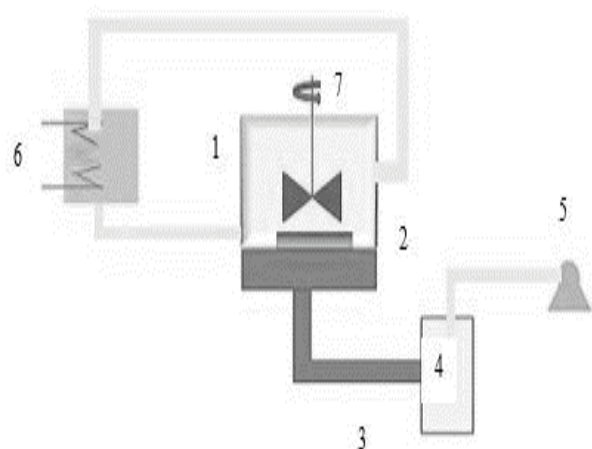


Fig. 2. (a) Schema of the device VMD: 1. Feed reservoir; 2. Membrane; 3. Permeate; 4. Condenser; 5. Vacuum pump; 6. Temperature control with heating oil; 7. Mixer and (b) VMD pilot [12].

partial flux J_i of the component i , can be calculated using Eq. (3):

$$J_i = \frac{m_i}{(A\Delta t)} \quad (3)$$

where m_i is the total mass of water vapor that permeates through the membrane, A is the effective membrane area, and Δt is the operation time. All VMD experiments were repeated at least two times to check the reproducibility of the measurements.

3. Results and discussion

3.1. Membrane hydrophobicity and roughness

Table 2 shows the properties of R-LDPE-alumina (R-LDPE- Al_2O_3) membrane prepared by TIPS method by using butyl acetate as a solvent.

It was clearly noticed that the obtained membrane has a hydrophobic character (115°) which is recommended for MD applications. Furthermore, there is a strong relationship between the roughness and the contact angle. According to Wenzel [21], the roughness enhances wettability and can be predicted using the Wenzel relation [(Eq. (4))]:

$$\cos\theta^* = r \cos\theta \quad (4)$$

where θ^* is the Wenzel contact angle, θ is the Young angle and r is the roughness ratio. Wenzel defined the roughness ratio as $r = a/A$, where a is the actual microscopic area and A is the apparent area [22].

If the factor r is larger than 1, a hydrophilic solid ($\theta < 90^\circ$) becomes more hydrophilic when rough ($\theta^* < \theta$). Conversely, a hydrophobic solid ($\theta > 90^\circ$) shows increased hydrophobicity ($\theta^* > \theta$).

For this reason, an atomic force microscope examined the topography of the surface of the obtained membrane. The atomic force microscopy (AFM) used, in this case, was carried out with a Nanoscope III device (Bruker, Santa Barbara, USA).

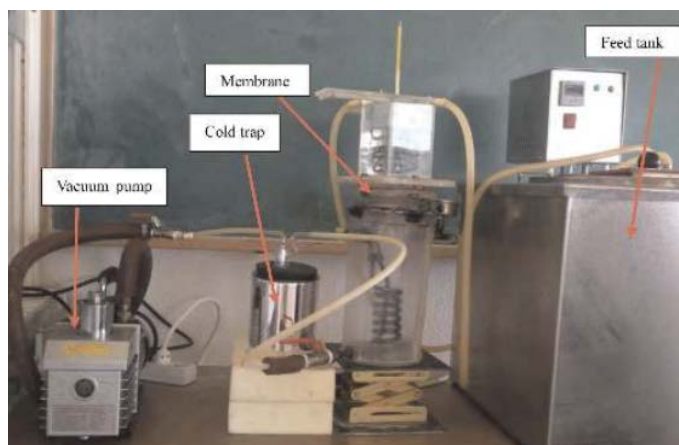


Table 2
Properties of the obtained membrane

Membrane proprieties	R-LDPE-alumina
Thickness (μm)	112 ± 0.005
Contact angle ($^\circ$)	115 ± 2
Roughness (nm)	527
Porosity (%)	65 ± 1.78
Pore size (μm)	0.1097
Bubble point pressure (bar)	0.593
Mechanical properties	
Mod (N/mm^2)	323.34
ϵ_{break} (%)	117.83

Fig. 3b illustrates the AFM image of the obtained membrane. The obtained membrane has the highest roughness of 527 nm.

3.2. Porosity, pore size and bubble point pressure

The porosity of the membrane is the ratio between the pore volume and the total volume of the membrane. When the porosity is high, the surface of the porous membrane for evaporation becomes higher. According to El-Bourawi et al. [23], the porosity of membrane in the MD varies from 30% to 85%. The value of the porosity of the obtained membrane presented in Table 2 equal to 65%. It can be concluded that the obtained membrane has a good porosity which can be applied in membrane distillation.

In Table 2, it can be observed that the pore size of the obtained membrane is equal to $0.1097 \mu\text{m}$. Generally, membranes with pore size between 100 nm to $1 \mu\text{m}$ are used in membrane distillation to avoid liquid penetration [24]. Generally, the pore size is an important parameter used to determine the vapor flux. When the pore size of the prepared R-LDPE-alumina membrane is high, the permeate flux becomes higher. Hence, it is necessary to find an optimum pore size for each MD process according to the operating conditions.

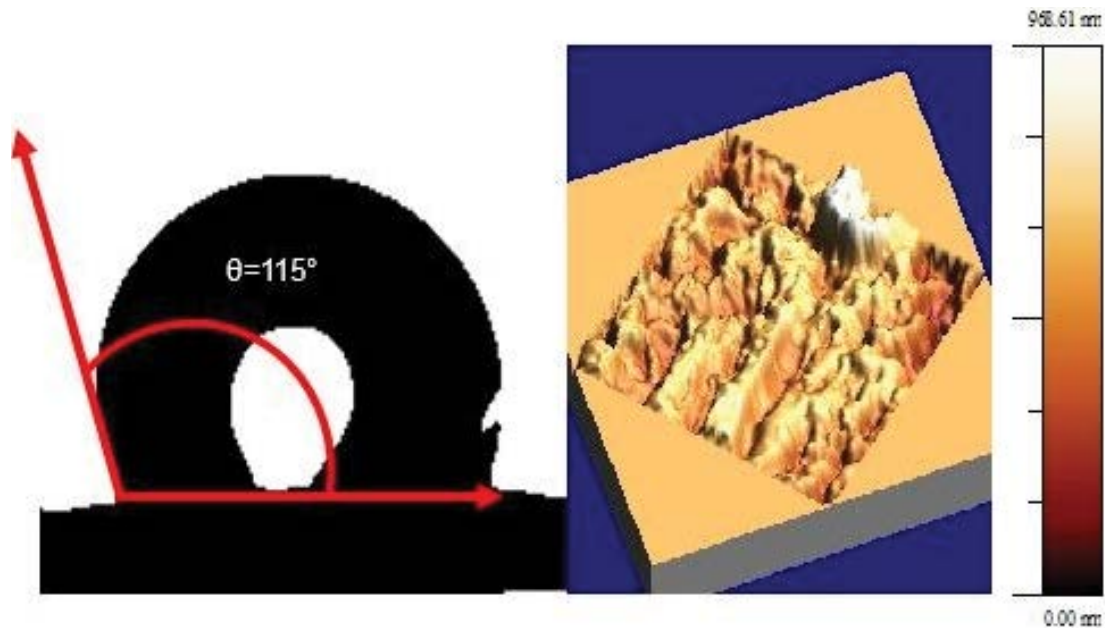


Fig. 3. (a) Contact angle of the obtained membrane and (b) atomic force microscopy image of the obtained membrane.

3.3. Membrane morphology

The morphology of the obtained membrane was characterized using SEM technique. SEM images of the top and the bottom of the surface of the obtained membrane are presented in Fig. 4.

Furthermore, Fig. 4 shows the SEM images of the cross-section of the obtained membrane. It was found that the obtained membrane has a leafy structure randomly oriented which revealed a porous nature of the obtained membrane. Also, it is observed that there is a presence of well stratified lamellae, which may be explained by the high degree of the crystallinity of the LDPE polymer. This agrees with Lloyd et al. [25], which reported that semi-crystalline and crystalline polymers can form folded chains and supra-molecular architectures such as axialites and spherulites.

This morphology was mainly due to the solid–liquid de-mixing, which occurred during the cooling of the film. According to Ji et al. [26], in fact, when the membranes are fabricated *via* TIPS, the majority of the solvents are rejected from the spherulites (matrix polymer) when the polymer is crystallized (if the crystallization temperature of the polymer is reached).

3.4. Mechanical properties

In general, the material stress-strain behavior can be calculated from the recorded forces and displacements based on the sample cross section area and loading mode [27]. Here, three samples ($1 \text{ cm}^2 \times 5 \text{ cm}^2$) were tested for each membrane. Each one was stressed, in unidirectional strain, at a constant rate of 5 mm/min. The result of the mechanical properties of the obtained flat sheet membrane (tensile strength, strain at break, elastic or Young's modulus and the breaking elongation) are presented in Table 2. It can be remarked that the obtained membrane has a high strain at

break (117%). As a result, it is very elastic and this may be because lamellae structure formed *via* the liquid–liquid phase separation process. Because the strain-induced micro-structural changes for membranes are often significant, invalidating many assumptions, such as in-plane elastic isotropy made about plastic deformation of bulk materials [28]. In addition, it had an important and applicable elastic modulus value. According to Wang et al. [28], the mechanical properties of membranes must be accurately analyzed in conjunction with the underlying mechanisms to optimize membrane design and processing for long service life.

3.5. Effects of feed temperature and transmembrane pressure

Fig. 5 shows the effect of the feed temperature and the transmembrane pressure on permeate flux. In fact, the permeate flux increases with increasing the feed temperature. It can be explained that the higher feed temperature results in higher water vapor pressure on the hot side of the membrane, resulting in a higher mass transfer force for penetration of the vapor, and this agrees with Wang et al. [29]. In addition, it can be observed that increasing the vacuum pressure results to increases the permeate flux. The vacuum pressure has an important role in VMD performance. For this reason, its effect on the permeate flux has been studied. In Fig. 5 it can be noticed that the permeate flux increase with decreasing of the vacuum pressure on the permeate side. This may be due to the significant increase in the vapor pressure difference between the feed and permeate side, which is the driving force. This result in agreement with Abdallah et al. [30].

3.6. Effect of feed water salinity

Fig. 6 shows clearly that the permeate flow rate decreases with increasing salinity (for 0.4 bar with 40 g/L salinity the

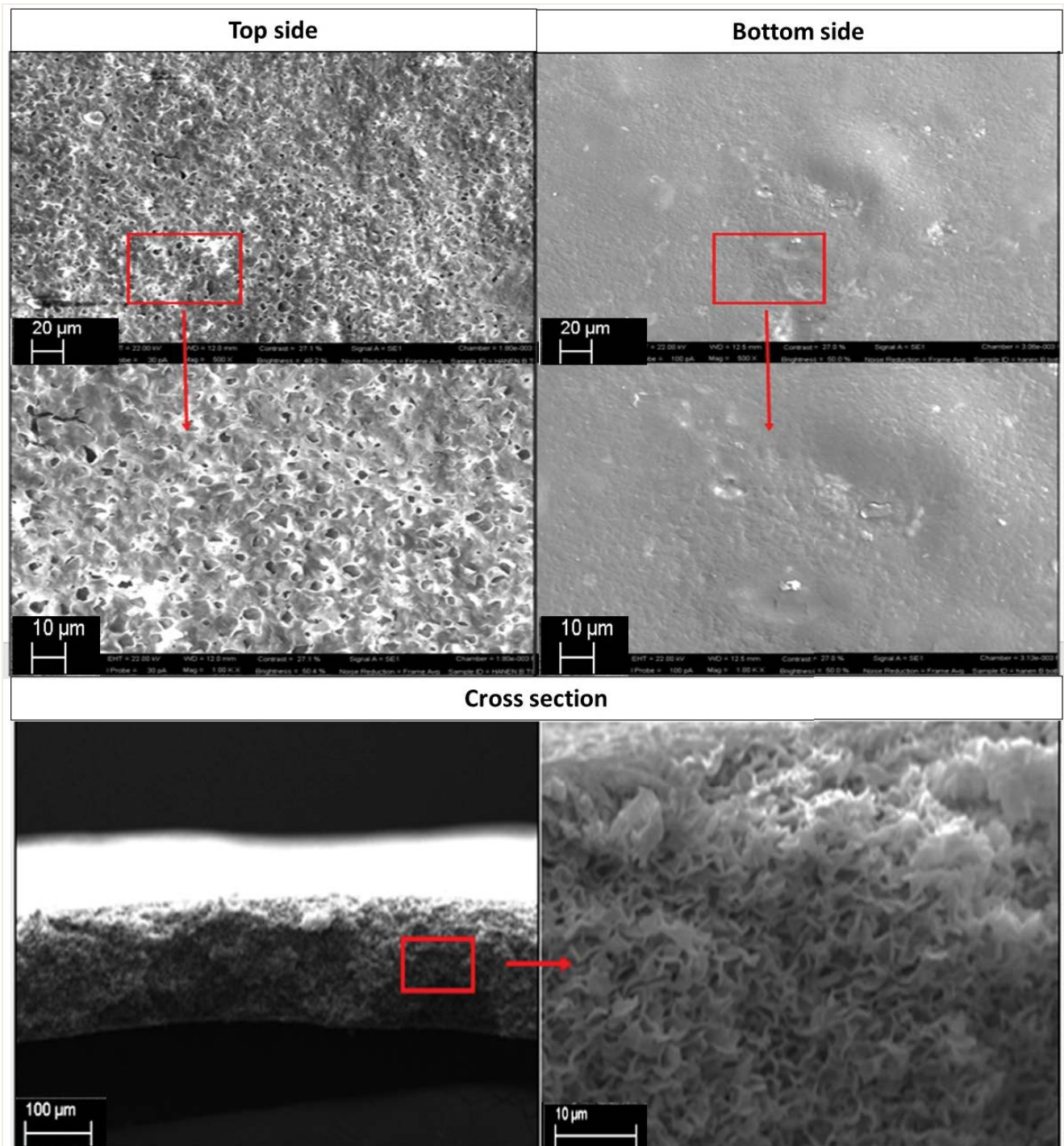


Fig. 4. Scanning electron microscopy image of the surface (top and bottom side) of the obtained membrane.

permeate flux is equal to 1.184 kg/hm² decrease to obtained 0.5 kg/hm² at the same pressure and the same salinity, this phenomenon decrease can be explained on one hand by the increasing of the partial vapor pressure at the inlet, on the other hand the increase in concentration polarization phenomena. The phenomenon of concentration polarization results from the fact that the solute concentration is greater to near the membrane than in the alimentation. A

resistance thus appears within a boundary layer formed in the power supply. This polarization phenomenon is modeled based on Fick's law.

3.7. Comparison of different membranes used in VMD

Table 3 shows the comparison of permeate flux of different membranes used in VMD found in the literature for

Table 3

Comparison of the VMD performance of different membranes found in the literature with the current R-LDPE-Al₂O₃ membrane

Membrane	PVDF	Polypropylene	ANN model	R-LDPE-alumina
Feed temperature (°C)	27	60	60	60
Vacuum pressure (bar)	0.0378	0.59	0.59	0.6
Permeate flux (kg/m ² ·h)	0.692	0.25	0.43	1.187
References	[32]	[30]	[33]	This study

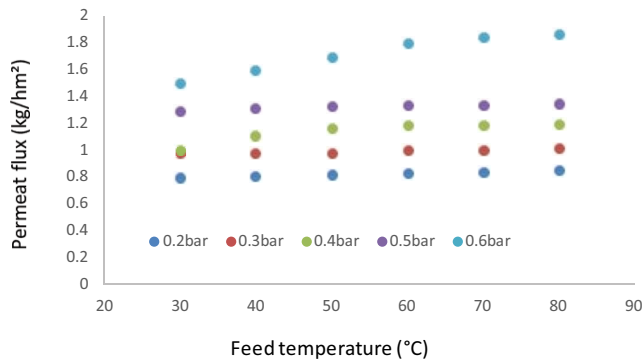


Fig. 5. Effect of the feed temperature and the transmembrane pressure on the permeate flux.

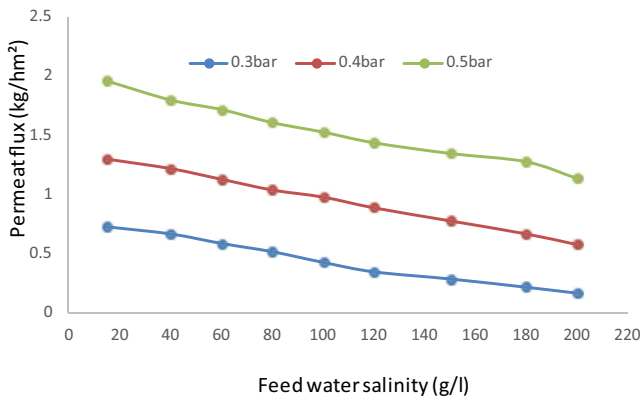


Fig. 6. Effect of feed water salinity.

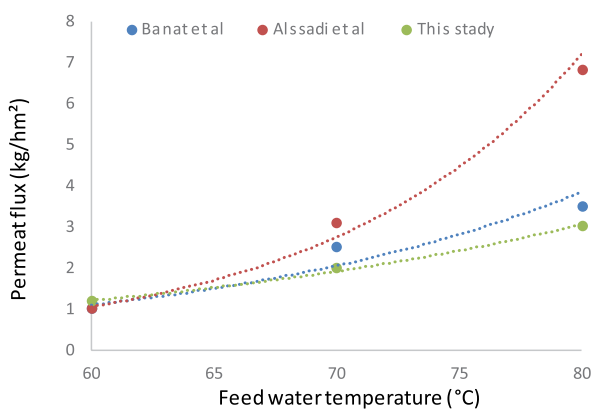


Fig. 7. Comparative study with Alsaadi et al. [32] and Banat et al. [32].

water desalination with the permeate flux obtained by the current work. By comparing the permeate flux obtained in this study by other studies, almost similar. This is an encouragement results because our starting polymer is recycled.

The comparison of the evolution of the permeate flow measured at different feed water temperatures it gives in Fig. 7. The results of Alsaadi et al. [31] and the work of Banat et al. [32] were used for this comparison. We can notice in Fig. 7 that our results are agree with the appearance given by Banat and Alsaadi and are closer to those of Banat et al. [32].

4. Conclusions

In this study, a novel composite flat sheet membrane was prepared, characterized, and then applied on the vacuum membrane distillation for desalination of the seawater and brackish water. In fact, based on a recycled polymer, which is the low-density polyethylene, it can be prepared a flat sheet membrane *via* the TIPS method using 8 wt.% of the R-LDPE in butyl acetate, adding 5% of the powder of alumina. The characterization of the obtained membrane shows that the obtained membrane has good proprieties such as the hydrophobicity, which has a contact angle, equals 115°, the porosity that equals 65% and the mechanical proprieties in terms of strain at break (equals 117%) which shows a good elasticity, moreover, it had an important and applicable elastic modulus value. In addition, the obtained membrane was tested in the vacuum membrane distillation and the result is promising because the permeate flux of the obtained membrane is similar than that found in literature.

Abbreviations

- PP — Polypropylene
- PE — Polyethylene
- PVDF — Polyvinylidene fluoride
- R-LDPE — Recycled low-density polyethylene
- TIPS — Thermally induced phase separation
- FTIR — Fourier-transform infrared spectroscopy
- CA — Contact angle
- RO — Reverse osmosis
- MD — Membrane distillation
- VMD — Vacuum membrane distillation
- SVMD — Solar vacuum membrane distillation
- Ra — Roughness
- Z (x, y) — Surface relative to the median plane
- Lx, Ly — Dimensions of the area
- θ* — Wenzel contact angle
- θ — Young angle
- r — Roughness ratio
- a — Actual microscopic area

References

- [1] J. Chang, J. Zuo, K.-J. Lu, T.-S. Chung, Membrane development and energy analysis of freeze desalination-vacuum membrane distillation hybrid systems powered by LNG regasification and solar energy, *Desalination*, 449 (2019) 16–25.
- [2] A. Hamzaoui, K. Hidouri, B. Chaouachi, Manufacture of Hydrophobic Membranes Using Recycled Polymers for the Brackish Water Distillation, 11th International Renewable Energy Congress (IREC), IEEE, Hammamet, Tunisia, 2020, pp. 1–6.
- [3] F. Khaled, K. Hidouri, B. Chaouach, Study of a developed model describing a vacuum membrane distillation unit coupled to solar energy, *World Acad. Sci. Eng. Technol., Int. J. Energy Pow. Eng.*, 13 (2019) 651–656.
- [4] R. Sarbatly, C.-K. Chiam, Evaluation of geothermal energy in desalination by vacuum membrane distillation, *Appl. Energy*, 112 (2013) 737–746.
- [5] N. Tang, Q. Jia, H. Zhang, J. Li, S. Cao, Preparation and morphological characterization of narrow pore size distributed polypropylene hydrophobic membranes for vacuum membrane distillation *via* thermally induced phase separation, *Desalination*, 256 (2010) 27–36.
- [6] A. Hamzaoui, K. Hidouri, B. Chaouachi, Comparative study of the performance of a locally manufactured membrane and the commercial one in vacuum membrane distillation of brackish water, *Desal. Water Treat.*, 247 (2022) 10–16.
- [7] A. Hanen, K. Fatma, A. Hiba, H. Khaoula, Ch. Bechir, A. Qusay, Novel composite membrane based on recycled low-density polyethylene-alumina used for vacuum membrane distillation, *Bull. Natl. Res. Cent.*, 47 (2023) 132, doi: 10.1186/s42269-023-01103-z.
- [8] M. Safavi, T. Mohammadi, High-salinity water desalination using VMD, *Chem. Eng. J.*, 149 (2009) 191–195.
- [9] J.-P. Mericq, S. Laborie, C. Cabassud, Vacuum membrane distillation of seawater reverse osmosis brines, *Water Res.*, 44 (2010) 5260–5273.
- [10] Z. Ding, L. Liu, M.S. El-Bourawi, R. Ma, Analysis of a solar-powered membrane distillation system, *Desalination*, 172 (2005) 27–40.
- [11] J. Koschikowski, M. Wiegand, M. Rommel, Solar thermal-driven desalination plants based on membrane distillation, *Desalination*, 156 (2003) 295–304.
- [12] F. Khaled, K. Hidouri, A. Criscuoli, B. Chouachi, Supply of solar energy in vacuum membrane distillation, *J. Ambient Energy*, 43 (2022) 2988–2999.
- [13] S. Al-Obaidani, E. Curcio, F. Macedonio, G. Di Profio, H. Al-Hinai, E. Drioli, Potential of membrane distillation in seawater desalination: thermal efficiency, sensitivity study and cost estimation, *J. Membr. Sci.*, 323 (2008) 85–98.
- [14] A. Akbari, R. Yegani, B. Pourabbas, A. Behboudi, Fabrication and study of fouling characteristics of HDPE/PEG grafted silica nanoparticles composite membrane for filtration of humic acid, *Chem. Eng. Res. Des.*, 109 (2016) 282–296.
- [15] Y. Jafarzadeh, R. Yegani, M. Sedaghat, Preparation, characterization and fouling analysis of ZnO/polyethylene hybrid membranes for collagen separation, *Chem. Eng. Res. Des.*, 94 (2015) 417–427.
- [16] C. Zhang, Y. Bai, Y. Sun, J. Gu, Y. Xu, Preparation of hydrophilic HDPE porous membranes *via* thermally induced phase separation by blending of amphiphilic PE-b-PEG copolymer, *J. Membr. Sci.*, 365 (2010) 216–224.
- [17] H. Strathmann, L. Giorno, E. Piacentini, E. Drioli, 1.4 Basic Aspects in Polymeric Membrane Preparation, E. Drioli, L. Giorno, Eds., *Comprehensive Membrane Science and Engineering*, Elsevier, Oxford, UK, 2017, pp. 65–84.
- [18] M. Pontié, C. Diawara, A. Lhassani, H. Dach, M. Rumeau, H. Buisson, J.C. Schrotter, Water defluoridation processes: a review. Application: nanofiltration (NF) for future large-scale pilot plants, *Adv. Fluorine Sci.*, 2 (2006) 49–80.
- [19] H. Ajari, B. Chaouachi, F. Galiano, T. Marino, F. Russo, A. Figoli, A novel approach for dissolving crystalline LDPE using non-toxic solvents for membranes preparation, *Int. J. Environ. Sci. Technol.*, 16 (2019) 5375–5386.
- [20] S. Fadhil, T. Marino, H.F. Makki, Q.F. Alsahly, S. Blefari, F. Macedonio, E. Di Nicolò, L. Giorno, E. Drioli, A. Figoli, Novel PVDF-HFP flat sheet membranes prepared by triethyl phosphate (TEP) solvent for direct contact membrane distillation, *Chem. Eng. Process. Process Intensif.*, 102 (2016) 16–26.
- [21] R.N. Wenzel, Resistance of solid surfaces to wetting by water, *Ind. Eng. Chem.*, 28 (1936) 988–994.
- [22] R.J. Good, M.K. Chaudhury, C. Yeung, A New Approach for Determining Roughness by Means of Contact Angles on Solids, *First International Congress on Adhesion Science and Technology*, CRC Press, Ooij, WJ, 2023, pp. 181–197.
- [23] M.S. El-Bourawi, Z. Ding, R. Ma, M. Khayet, A framework for better understanding membrane distillation separation process, *J. Membr. Sci.*, 285 (2006) 4–29.
- [24] K.W. Lawson, D.R. Lloyd, Membrane distillation, *J. Membr. Sci.*, 124 (1997) 1–25.
- [25] D.R. Lloyd, K.E. Kinzer, H.S. Tseng, Microporous membrane formation *via* thermally induced phase separation. I. Solid-liquid phase separation, *J. Membr. Sci.*, 52 (1990) 239–261.
- [26] G.-L. Ji, L.-P. Zhu, B.-K. Zhu, C.-F. Zhang, Y.-Y. Xu, Structure formation and characterization of PVDF hollow fiber membrane prepared *via* TIPS with diluent mixture, *J. Membr. Sci.*, 319 (2008) 264–270.
- [27] R.P. Vinci, J.J. Vlassak, Mechanical behavior of thin films, *Annu. Rev. Mater. Sci.*, 26 (1996) 431–462.
- [28] K. Wang, A.A. Abdalla, M.A. Khaleel, N. Hilal, M.K. Khraisheh, Mechanical properties of water desalination and wastewater treatment membranes, *Desalination*, 401 (2017) 190–205.
- [29] Y. Wang, Z. Xu, N. Lior, H. Zeng, An experimental study of solar thermal vacuum membrane distillation desalination, *Desal. Water Treat.*, 53 (2015) 887–897.
- [30] H. Abdallah, A.F. Moustafa, A.A. AlAnezi, H.E.M. El-Sayed, Performance of a newly developed titanium oxide nanotubes/polyethersulfone blend membrane for water desalination using vacuum membrane distillation, *Desalination*, 346 (2014) 30–36.
- [31] A.S. Alsaadi, S. Ghaffour, J.-D. Li, S. Gray, L. Francis, H. Maab, G.L. Amy, Modeling of air-gap membrane distillation process: a theoretical and experimental study, *J. Membr. Sci.*, 445 (2013) 53–65.
- [32] F. Banat, F.A. Al-Rub, K. Bani-Melhem, Desalination by vacuum membrane distillation: sensitivity analysis, *Sep. Purif. Technol.*, 33 (2003) 75–87.